VIII. NUCLEAR MAGNETIC RESONANCE AND HYPERFINE STRUCTURE

Prof. F. Bitter
Prof. J. S. Waugh
Dr. L. C. Bradley III
Dr. H. H. Stroke
Dr. J. F. Waymouth
T. Fohl
R. L. Fork
J. V. Gaven, Jr.
W. D. Halverson
E. R. Hegblom
Ilana Levitan
F. A. Liégeois
J. D. Macomber
F. Mannis
I. G. McWilliams
P. G. Mennitt
S. R. Miller
H. C. Praddaude
O. Redi
C. J. Schuler, Jr.
W. W. Smith
W. J. Tomlinson
W. T. Walter

RESEARCH OBJECTIVES

The aims of this group are threefold: first, the investigation of molecular and solid-state problems by nuclear magnetic-resonance techniques; second, the investigation of the structure of atomic nuclei, particularly of radioactive nuclei, by nuclear magnetic-resonance techniques and by the investigation of atomic hyperfine structure and isotope shift; third, the investigation of spectroscopic light sources and mercury-rare-gas plasmas, generally, with particular emphasis on the study of collision processes, interaction with high magnetic fields, and coherence properties of the radiating atoms.

In order to obtain information from the relatively small numbers of atoms with radioactive nuclei that can be prepared, this group has placed an emphasis on the optical properties of atomic vapors. In addition to straightforward spectroscopic investigations that make use of gratings and interferometers, and especially designed light sources requiring very few atoms, techniques have been developed for eliminating Doppler broadening, especially through the use of radiofrequency and microwave absorption, and also of atomic-beam light sources.

A synopsis of our recent work reflects these aims. Optical pumping and nuclear resonance were successfully achieved for the first time in a radioactive isotope. The results of our isotope-shift experiments show that further systematic study of both isotope and nuclear isomer shifts gives promise of yielding valuable information on nuclear interactions. A theoretical study was made of the "hyperfine-structure anomaly" and a formalism has been developed by which we can test explicitly assignments of nuclear wave functions. Hyperfine-structure "level crossing" and double-resonance experiments have been carried out with both stable and radioactive atoms. Further work with both types of experiments is expected to yield data on atomic collisions and radiation coherence. An experiment has been performed to test possible parity nonconservation in molecular interactions. This work is being extended to other transitions, and to refining the upper limit on the mixing coefficient of a parity nonconserving state. The construction of a spherical discharge tube, 2 feet in diameter, has permitted the study of a mercury-rare-gas plasma under a condition that minimizes the effects of wall collisions. Related theoretical and experimental work is continuing. We have also constructed a new double-resonance, magnetic-scanning apparatus with greatly increased magnet homogeneity, and a new grating mirror monochromator, of 36-ft focal length, for the high-resolution spectroscopic work.

Our molecular studies by means of nuclear resonance continue to emphasize: (a) the nature of phase transitions, particularly those involving order-disorder phenomena, in solids; (b) intermolecular forces, including their reflection in the transport properties of fluids; and (c) determination of the structures of simple molecules.

F. Bitter, L. C. Bradley III, H. H. Stroke, J. S. Waugh

A. SELF-DIFFUSION IN LIQUID METHANE AND ETHANE

The self-diffusion coefficient D for liquid CH_4 has been measured at 1 atm over the normal liquid range, by using a spin-echo technique. The results may be expressed as

$$D = 80.5 \times 10^{-5} \exp(-337/T) \text{ cm}^2 \text{ sec}^{-1}, \quad 94°K \leq T \leq 111°K.$$

The constancy of the activation energy, 0.67 kcal/mole, over such a small temperature range is not surprising. A comparison of the reduced diffusion constant

$$D_R = D M^{1/2} P_c^{1/3} T_c^{-5/6},$$

where M is the molecular weight and P_c and T_c are critical constants, with similar results for argon[1,2] gives agreement within combined experimental error, as expected from the principle of corresponding states.

The results for C_2H_6 are much more interesting, inasmuch as they cover the very wide temperature range along the vapor-liquid curve from the triple point to the critical point. A plot of $\ell n D$ vs $1/T$ is strongly concave upward. Among simple schemes for describing transport processes in fluids, a fit with the experimental points could be obtained either with a pure free-volume expression similar to that which is found empirically to hold for viscosities[3]:

$$D = 104 \times 10^{-5} \exp\left(\frac{1.56\rho}{\rho - 0.85}\right) \text{ cm}^2 \text{ sec}^{-1}$$

or with a modified free-volume theory of the type proposed by Cohen and Turnbull[4]:

$$D = 5.06 \times 10^{-5} T^{1/2} \exp\left(\frac{1.37\rho}{\rho - 0.85}\right) \text{ cm}^2 \text{ sec}^{-1}.$$

Here, ρ is the density, whose hypothetical value at T = 0, 0.85 gm cm^{-3}, is consistent with various estimates that can be made for C_2H_6 from a variety of experimental facts.

Fessenden and Schuler[5] have measured the steady-state intensity of the paramagnetic resonance absorption of ethyl radicals in a sample of liquid ethane undergoing electron bombardment. Their estimate of the recombination rate constant k_D for the radicals at 135°K, $k_D = 4 \times 10^9$ ℓ mole^{-1} sec^{-1}, may be compared with our measurements if ethyl radicals are assumed to diffuse at the same rate as ethane molecules and if the recombination reaction is controlled by diffusion so that the Smoluchowski equation[6] can be applied:

$$k_D = 8\pi N D \sigma \times 10^{-3} \ \ell \text{ mole}^{-1} \text{ sec}^{-1}.$$

Inserting our diffusion constant at 135°K and taking a hard sphere diameter σ of 4.0 Å from gas-phase viscosity and PVT measurements, we predict $k_D = 11 \times 10^9$ ℓ mole^{-1} sec^{-1}. This result is in satisfactory agreement with the rough value of Fessenden and Schuler, particularly when it is considered that no account is taken in the Smoluchowski equation of the fact that ethyl radicals probably do not recombine unless they come together in a suitable relative orientation. Professor W. H. Stockmayer collaborated in this work.

We are now preparing to determine the dependence of D on T at constant volume for C_2H_6 and some other liquids, in order to distinguish between the above-mentioned formulas and to throw light on the nature of transport phenomena in general. The experiment will involve spin-echo measurements of D as a function of T and P up to several thousand atmospheres.

J. V. Gaven, Jr., J. S. Waugh

References

1. J. W. Corbett and J. H. Wang, J. Chem. Phys. 25, 422 (1956).
2. G. Cini-Castagnoli and F. P. Ricci, J. Chem. Phys. 32, 19 (1960); Nuovo cimento 15, 795 (1960).
3. A. K. Doolittle and D. B. Doolittle, J. Appl. Phys. 28, 901 (1957).
4. M. H. Cohen and D. J. Turnbull, J. Chem. Phys. 31, 1164 (1959).
5. R. W. Fessenden and C. H. Schuler, Jr., J. Chem. Phys. 33, 935 (1960).
6. M. V. Smoluchowski, Z. physik. Chem. 92, 129 (1917).

B. "SELECTION RULES" FOR ROTATIONAL INELASTIC SCATTERING

Nuclear relaxation in relatively dilute polyatomic gases arises from the fluctuation of intramolecular perturbations, which is brought about by collisions that change the rotational state of the molecule. Relaxation measurements thus afford a means of studying the anisotropy of intermolecular forces.[1,2] In H_2, and probably in other molecules as well, the important collisional process is one that changes the rotational magnetic quantum number m_J, but not the total angular momentum $J\hbar$. A rather elaborate scattering theory, or its equivalent,[1] is necessary to relate fully the intermolecular potential to nuclear relaxation times, but certain properties of the potential can be deduced more easily. For example, in a diatomic molecule in the rotational level J = 1, the relative collisional transition probabilities per unit time W_1 for $\Delta m_J = \pm 1$, and W_2 for $\Delta m_J = \pm 2$, are related to the symmetry of the intermolecular force and, in principle, are measurable separately. For the molecule HD, specifically, the nuclear transverse relaxation times T_2 for J = 1 can be shown[2] to be

$$\left(\frac{1}{T_2}\right)_H = \frac{4\gamma_H^2 H'^2_H}{3(W_1+2W_2)} + \frac{16\gamma_H^2\gamma_D^2\hbar^2}{45r_{HD}^6 W_1}$$

$$\left(\frac{1}{T_2}\right)_D = \frac{4\gamma_D^2 H'^2_D}{3(W_1+2W_2)} + \frac{2\gamma_H^2\gamma_D^2\hbar^2}{15r_{HD}^6 W_1} + \frac{(eqQ_D)^2}{20\hbar^2 W_1}.$$

Here, the subscripts H and D refer to the proton and deuteron, respectively, γ is a

gyromagnetic ratio, r an internuclear distance, and eqQ a quadrupole coupling constant. Insertion of numerical values shows that the proton relaxes 11 times faster than the deuteron if $W_1 = W_2$, and 20 times faster if $W_2 = 0$. The appropriate experiments are now in progress.

J. S. Waugh

References

1. I. Oppenheim and M. Bloom, Can. J. Phys. 39, 845 (1961).
2. C. S. Johnson and J. S. Waugh, J. Chem. Phys. (in press).

C. HYPERFINE STRUCTURE AND ISOTOPE SHIFT IN Hg^{195} AND Hg^{195*}

An experiment is under way to measure the hyperfine structure and isotope shift in Hg^{195} and its isomeric state Hg^{195*}. This experiment is similar to that performed on Hg^{197} and Hg^{197*}.[1] The mercury will be produced by the reaction Au^{197} (p, 3n) Hg^{195}. Examination of the gamma-ray spectra from trial bombardments has led to the excitation curve for the reaction, and enabled us to select the bombardment energy that maximizes the yield of Hg^{195}, and minimizes the yield of Hg^{197}. It is estimated that a 12-hour bombardment will yield approximately 5×10^{13} atoms of Hg^{195*}, and approximately twice that many atoms of Hg^{195}. The ratio of Hg^{195*} to Hg^{197*} is 12:1 approximately.

W. J. Tomlinson III, H. H. Stroke

References

1. A. C. Melissinos and S. P. Davis, Phys. Rev. 115, 130 (1959).

D. STUDY OF D-C DISCHARGES IN A LARGE, SPHERICAL VESSEL

The spherical tube shown in Fig. VIII-1 is constructed of Pyrex, and is mounted on a vacuum system consisting of a three-stage oil-diffusion pump and a forepump. A large furnace may be lowered over the body of the tube for baking.

The anode is a sphere of copper, approximately 25 mm in diameter. It is mounted on a stainless-steel rod that is shielded by a glass tube. The rod projects from an iron slug through which the anode is moved by means of an external magnetic field. The cathode is a group of three oxide-coated coils mounted in parallel on two rods that pass through a magnetic slug, and connect to two leads of copper braid. The probes are tungsten discs mounted on long, glass-shielded rods that are connected to magnetic slugs.

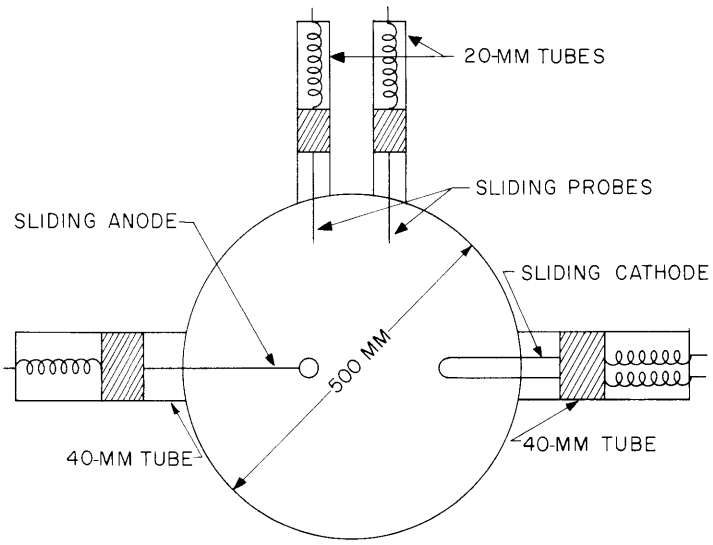

Fig. VIII-1. Top view of the spherical discharge vessel.

Preliminary experiments have been performed in a mixture of argon and mercury vapor. The pressure is measured by means of an Autovac gauge. The mercury vapor pressure is determined by the temperature of the tube walls, which is approximately 25°C.

The appearance of the discharge at various pressures is illustrated by the photographs shown in Fig. VIII-2. Figure VIII-2a shows the discharge with the anode and cathode approximately 10 cm apart and an argon pressure of 5 mm Hg. In Fig. VIII-2b the distance between electrodes is 14 cm, and the pressure is 3 mm Hg. Figure VIII-2c and VIII-2d shows the discharge when the pressure is 2 mm Hg and 1.7 mm Hg, respectively, and the separation of the electrode is 14 cm. The current is 2 amps in all cases.

As can be seen, the dimensions of the dark region between the cathode glow and the "plasma glow" increase at the expense of the "plasma glow" with decreasing pressure until the condition in Fig. VIII-2d is reached. In that mode there is only a thin sheath of excited atoms around the anode. The size of the cathode glow increases with decreasing pressure.

Langmuir probe measurements indicate that the electrons have a non-Maxwellian energy distribution in the "plasma glow," and a Maxwellian distribution in the dark space.

It is believed that in discharges in which the anode is in the cathode region and no plasma column develops the diffusion current of the electrons is more than sufficient to carry the tube current. In this case a region of null or negative electric field occurs between the anode and the edge of the cathode glow.[1] In a tube of this geometry, operation in this mode should result in the cathode glow acting as a spherical source of ions

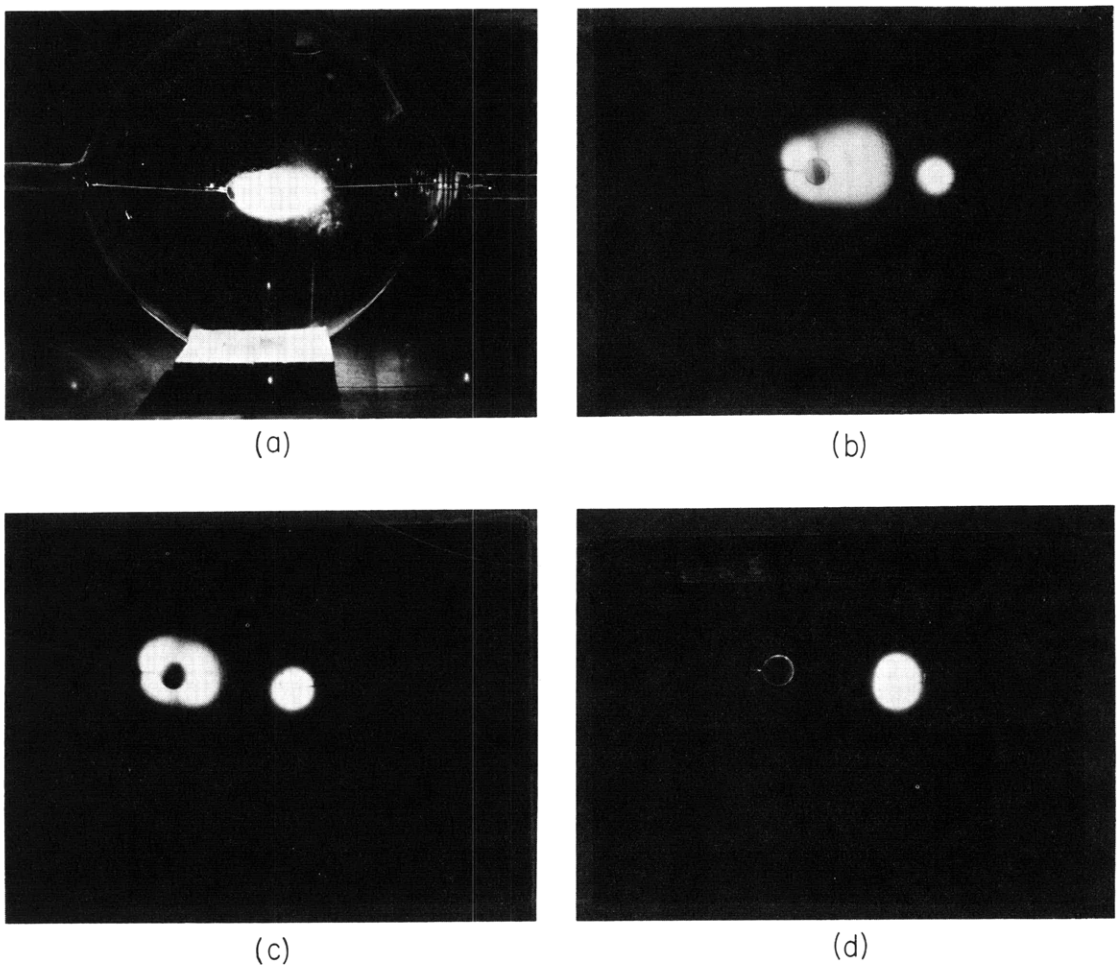

Fig. VIII-2. Mercury-argon discharge (cathode at right in each part): (a) pressure, 5 mm Hg; (b) pressure, 3 mm Hg; (c) pressure, 2 mm Hg; (d) pressure, 1.7 mm Hg.

and electrons that diffuse radially. Experiments are in progress which should determine to what extent this is so.

The density of electrons in the region between the cathode glow and the walls should be proportional to the inverse of the radial distance from the center, if no recombination or ionization is present. Deviations from this situation will indicate that some source or sink of particles is in the region, and we hope that a study of these deviations will yield information about the recombination coefficients involved.

T. Fohl

References

1. M. J. Druyvesteyn and F. N. Penning, Revs. Modern Phys. 12, 87 (1940).

E. THE PERTURBATION OF A PLASMA BY A PROBE

An analysis of the perturbation of electron density and plasma potential by a Langmuir probe has been carried out for a spherical probe in the center of a spherical discharge tube. This consists of a solution in the ambipolar limit of the transport equations for electrons and ions separately in the plasma, matched with the sheath equations for electrons and ions at the probe. To simplify the analysis, the sheath equations for a plane probe were used; hence the results are strictly valid only for the case in which the sheath thickness is small as compared with the probe radius.

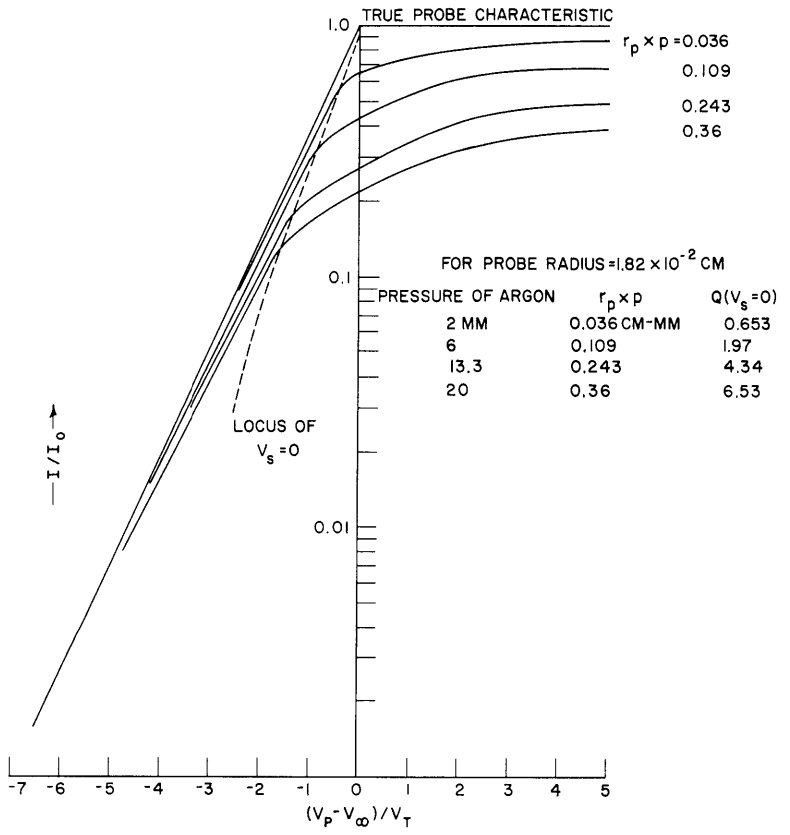

Fig. VIII-3. Calculated electron current vs probe voltage characteristics for various values of $Q(V_S=0)$. "True Probe Characteristic" is that obtained for no perturbation (pressure very small so that $Q \approx 0$).

If n_1 is defined as the electron density in the plasma at the sheath boundary, n_o as the electron density in the plasma in the absence of a probe, and ΔV as the change in plasma potential caused by the presence of the probe, then

$$\left.\begin{aligned} \frac{n_p}{n_o} &= \frac{1}{1+Q} \\ \Delta V &= -\frac{kT_e}{e}\left(1-\frac{Q_e}{Q}\right)\ln(1+Q) \end{aligned}\right\} \qquad (1)$$

where T_e is the electron temperature and

$$Q = Q_e + Q_i$$

$$Q_e = \frac{r_p}{D_e}\sqrt{\frac{kT_e}{\pi m_e}}\, e^{eV_s/kT_e} \qquad V_s < 0$$

$$= \frac{r_p}{D_e}\sqrt{\frac{kT_e}{\pi m_e}} \qquad V_s > 0$$

$$Q_i = \frac{r_p}{D_a}\sqrt{\frac{kT_i}{\pi m_i}}\, e^{-eV_s/kT_i} \qquad V_s > 0$$

$$= \frac{r_p}{D_a}\sqrt{\frac{kT_i}{\pi m_i}} \qquad V_s < 0 .$$

Here r_p is the probe radius; D_a, the ambipolar diffusion coefficient; D_e, the electron diffusion coefficient; and V_s, the potential difference across the sheath (V_s is positive when the probe is positive with respect to the plasma). Since both Q_e and Q_i are functions of sheath voltage, the perturbation of electron density and plasma potential will also be functions of sheath voltage. Thus, the probe characteristic will also be distorted. Figure VIII-3 shows calculated characteristics for various values of probe radius multiplied by pressure (which determines Q) for a mercury plasma in a buffer gas of argon. For simplicity, the ion temperature at the sheath edge was taken to be equal to the electron temperature. Note that, for the larger values of Q, not only are electron density and plasma potential considerably altered, but it becomes increasingly difficult to identify the point of zero sheath voltage.

Analysis of the case for a plane probe in a cylindrical discharge tube, with and without an axial magnetic field, is also being carried out. Results, thus far, indicate that, except for a numerical factor believed to be approximately 1, the perturbation of electron density is the same as that given by Eq. 1, provided that Q is multiplied by a factor $1 + \mu_e\mu_i B^2$. This suggests that the perturbations are not very sensitive to the ratio of sheath thickness to probe radius; and that Eq. 1 may be more general than is expected. However, the detailed shape of the probe characteristics shown in Fig. VIII-3 can apply only when the sheath thickness is small compared with probe radius.

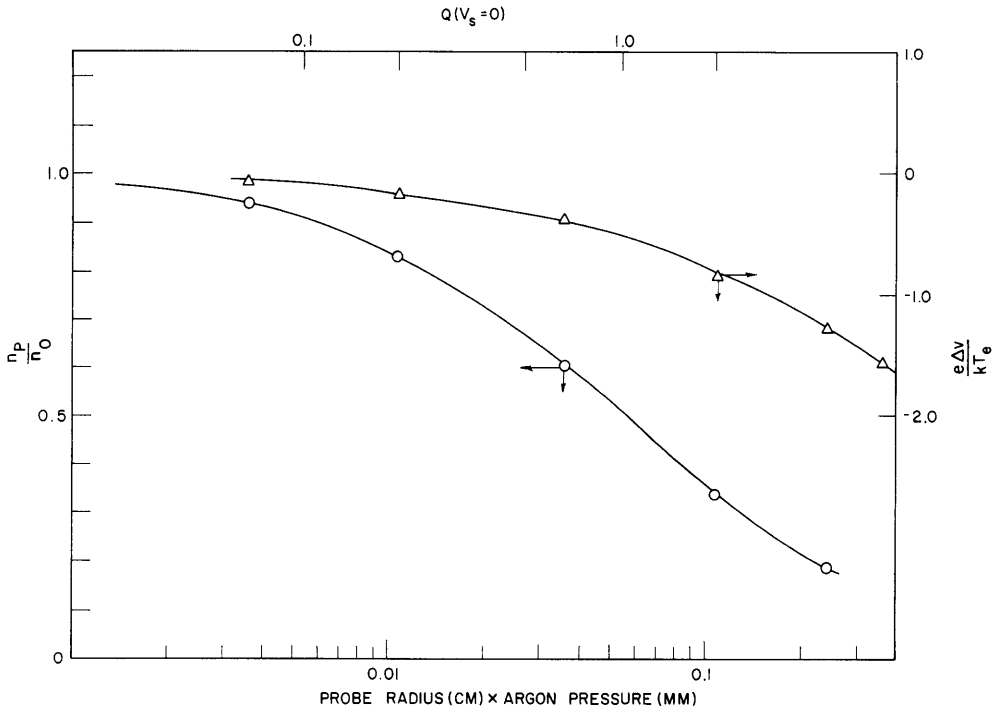

Fig. VIII-4. Perturbation of plasma density and potential at zero sheath potential V_s vs $Q(V_s=0)$ as determined by probe radius times pressure. (n_p is the electron density determined from random electron current to the probe at zero sheath potential; n_o is the electron density in the absence of the probe; ΔV is the difference between probe potential at zero sheath potential and the plasma potential in the absence of the probe.)

Figure VIII-4 shows calculated values of n_1/n_o and $\frac{e\Delta V}{kT_e}$ versus $Q(V_s=0)$ and $r_p \times p$. Examination of the expression for Q will show that for $V_s = 0$, Q is essentially the sum of the ratios of probe radius to electron mean-free path and probe radius to ion mean-free path. Thus these results agree with those from earlier work that the important parameter is the ratio of probe radius to mean-free path. Note, however, that even for $Q(V_s=0)$ equal to 0.1, the perturbation in electron density is 10 per cent.

J. F. Waymouth